Deexcitation of fragments produced in deeply inelastic collisions of 100 MeV ^{16}O with ^{27}Al

G. R. Young,* K. A. Van Bibber,† A. J. Lazzarini,‡ and S. G. Steadman
Laboratory for Nuclear Science and Physics Department, Massachusetts Institute of Technology, Cambridge, Massachusetts 02139

F. Videbæk
Laboratory for Nuclear Science, Massachusetts Institute of Technology, Cambridge, Massachusetts 02139 and The Niels Bohr Institute, University of Copenhagen, DK-2100 Copenhagen Ø, Denmark

(Received 20 April 1981)

A study has been made of the γ-ray deexcitation following deeply inelastic collisions between 100 MeV ^{16}O and ^{27}Al. An experimental apparatus including a gas proportional particle telescope, a Ge(Li) detector, and three NaI(Tl) detectors was used. All possible particle-γ and particle-multiple-γ coincidences for projectilelike fragments with $Z \geq 3$ were recorded. Yields and anisotropies of several discrete transitions were measured, as well as the mean and width of the gross multiplicity distribution as a function of detected Z and reaction inelasticity. Estimates of average γ-ray transition energy, average energy carried by γ-ray deexcitation, and the degree of side feeding in observed γ cascades were made. Observed anisotropies are consistent with considerable fragment spin alignment being present. Values of mean γ-ray multiplicity never exceed simple sticking model predictions; particle emission effects are seen to be important. The summed radiative strength of observed discrete line transitions is found to be less than unity, sometimes considerably so, for most deeply inelastic collisions. A short discussion is given of insights obtained on the entry state distribution for γ-ray emission and of the results of statistical model calculations of the relative yields of observed final states.

NUCLEAR REACTIONS $^{27}Al(^{16}O,X\gamma)$, $E=100$ MeV; measured X-γ coinc, Ge(Li) detector; measured X-γ-γ multiplicity, Ge(Li), NaI detectors; deduced decay product yields, alignment, radiative strengths, γ multiplicity mean and width.

I. INTRODUCTION

Several types of coincidence experiments studying deeply inelastic collisions (DIC) have been performed in order to extend the understanding of such strongly damped collisions and in particular to probe the role of angular momentum in these reactions. Among the quantities measured are heavy particle-heavy particle correlations,[1-4] heavy particle-light particle correlations,[5-7] total γ-ray multiplicity distributions for various projectilelike fragments,[8-12] and the circular polarization of the γ rays emitted by the targetlike fragment.[13]

From these experiments several features of DIC have been observed. The final state is predominantly two-body in nature before particle emission and a possible fissioning[1] of a heavy targetlike fragment. Energetic α emission accompanies a large fraction of certain projectilelike fragments.[5-7] The mean γ-ray multiplicity[8-12] is consistent with predictions of simple models such as the peripheral sticking model of Tsang[14] for tangential friction. The γ rays emitted display sizable values of circular polarization[13] and have angular correlations with projectilelike fragments[15-17] that suggest a considerable fragment spin alignment perpendicular to the reaction plane. Neutron-heavy ion coincidence measurements,[18-20] at least for heavier systems at center-of-mass energies 1.2-2 times the Coulomb barrier, are consistent with the final composite system being in a state of statistical equilibrium.

The measurements reported herein were designed to study the γ-ray deexcitation step in DIC in one system in a detailed way, with a view toward ad-

dressing the following questions where possible: (1) How is the intrinsic angular momentum of the dinuclear complex shared between the fragments? (2) What are the entry states for the reaction after particle emission? (3) Are the spins of the fragments aligned as expected in a classical, peripheral model of DIC? How is the observed alignment affected by light particle emission? (4) How much of the initial orbital angular momentum, which can range up to several tens of $\hbar$, is transferred to intrinsic spin?

To study the above questions, measurements were made to examine the γ-ray deexcitation step following DIC between 100 MeV ^{16}O projectiles and ^{27}Al targets. In the experiment, projectilelike fragments were detected over a 10° angular range at a mean angle beyond the classical grazing angle and were classified by energy, Z, and angle. γ rays were detected in coincidence with heavy ions in two modes, the first being a high resolution mode employing a Ge(Li) detector to identify discrete transitions, the second being a low resolution mode employing an array of NaI(Tl) detectors to obtain moments of the γ-ray multiplicity distribution. Yields for discrete transitions were used to study side feeding behavior in γ-ray cascades, variation of particle-γ ray anisotropy and thus spin alignment with light particle emission, and the fraction of DIC events which decay by observed γ-ray transitions.

The method chosen provides a good means to study the total angular momentum and excitation energy carried by γ-ray emission, the alignment of fragment spin after particle emission, the location of entry states for γ-ray emission, and the variation of these quantities with fragment Z and reaction inelasticity. Extraction of information on the distribution of entrance channel partial waves involved in DIC,[12,21] or the fragment total spins and entry state distributions,[22,23] is hampered by incomplete knowledge of, in particular, the effects of particle emission from either fragment.

The fusion[24–26] and DIC[27] cross sections have been measured for the ^{16}O+^{27}Al system at 100 MeV and give a cross section $\sigma_R = 1700$ mb and $\sigma_{fus} = 1050$ mb. A sharp cutoff model partial wave decomposition of σ_R at 100 MeV (Ref. 27) (see Table I) yields a narrow range of partial waves (31–37 $\hbar$) in a peripheral picture for DIC for the system and also shows $\sigma_{DIC}/\sigma_R \sim \frac{1}{3}$ at 100 MeV. Isotope distributions for projectilelike fragments were measured earlier in a time-of-flight experiment[28] (see Fig. 1), enabling one to tentatively identify final systems from the fragment Z-discrete γ coincidences recorded. As the laboratory grazing angle is 10° at 100 MeV, it is straightforward to record particle-γ coincidences with good efficiency for a mean particle angle much larger than the grazing angle. This is important to reduce the number of detected fusion-evaporation events. The lightness of the system means few Z channels are dominant and each has a narrow mass distribution (3–4 u). The number of low-lying nuclear levels is few, and they are well known. Thus, collection of sufficient counts per channel is possible in a reasonable length of time.

TABLE I. Total cross sections and sharp cutoff l values for evaporation residues, deeply inelastic events and quasielastic events for 100 MeV ^{16}O+^{27}Al. (After Ref. 27.)

$E_{lab}(^{16}O)$	100 MeV
$E_x(^{43}Sc)$	75.9 MeV
σ_{ER}[a]	1035 ±200 mb
l_{cr}	30.5±3$\hbar$
σ_{DIC}	481 ± 50 mb
Δl_{DIC}	6.5$\hbar$
σ_{QE}	174 ± 30 mb
σ_R	1690 ±210 mb
	1770 ±200 mb[b]
l_R	39.3± 2.5$\hbar$[c]
	40 ± 2$\hbar$[b]

[a]Interpolated from Ref. 25.
[b]From quarter point analysis of elastic scattering.
[c]From optical model fit to elastic scattering.

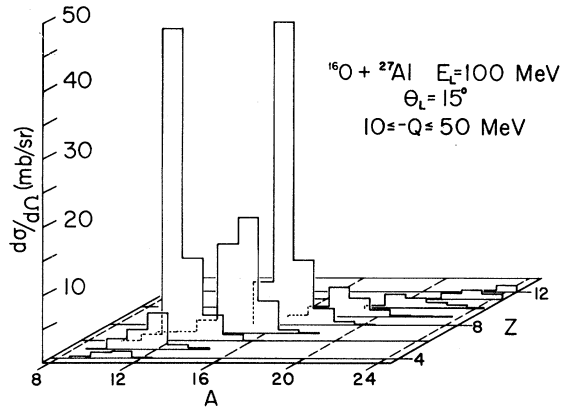

FIG. 1. Yields for the various nuclides produced in DIC of 100 MeV ^{16}O+^{27}Al, as determined using a time-of-flight spectrometer, summed over the range of inelasticities $10 \leq -Q \leq 50$ MeV. The strongest yields are found for ^{12}C and ^{16}O.

The experiment is described in Sec. II, and results for particle-discrete γ and particle-γ multiplicity measurements are given in Sec. III. Discussions of yield curves, anisotropies, computation of particle-γ correlations, and multiplicity distributions are given in Sec. IV. A summary of the results together with suggestions for further work are given in the last section.

II. EXPERIMENT

A. Method

All experiments reported here involved counting particle-γ ray coincidences resulting from reactions between 100 MeV ^{16}O projectiles and ^{27}Al and were carried out at the Brookhaven National Laboratory Tandem Van de Graaff facility. Earlier measurements of the mass and Z spectra from $^{16}O+^{27}Al$ collisions by our group have been reported in Refs. 27 and 28 and form a partial basis of results for the present work.

A schematic diagram of the experimental apparatus is shown in Fig. 2. No slits were used in the beam line in order to reduce γ-ray background. Beams, typically of 100 e nA, were checked for correct optics by viewing a quartz target periodically during the experiment. Targets were $>99.9\%$ pure ^{27}Al of nominal thickness 150 μg/cm^2. Contamination of the target due, e.g., to carbon buildup, was checked by comparing singles spectra measured for various particle groups to those measured earlier using a time-of-flight (TOF) spectrometer and known to be free of contaminant problems. The results indicated a contamination of the particle spectra of at most 15% and only for $-Q>50$ MeV.

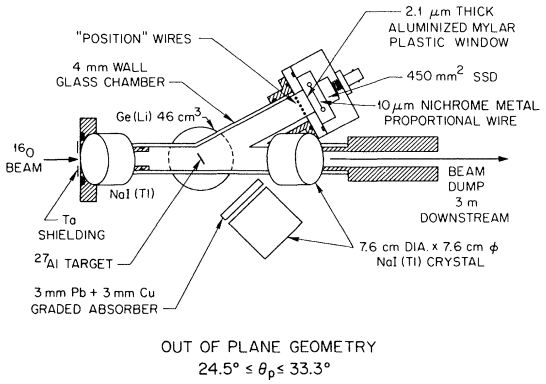

FIG. 2. Schematic diagram of apparatus used in the particle-gamma coincidence experiments.

Gamma rays were detected with high resolution in a 45 cm^3 Ge(Li) detector which had a resolution of 2.4 keV for 1332 keV γ rays and was 8% efficient relative to a 7.6×7.6 cm ϕ NaI(Tl) detector for such γ rays. The energy dependence of the full-energy-peak efficiency for the Ge(Li) detector was measured using several calibrated reference sources placed at the target position. Count rates up to 35 kcps were allowed, resulting in a line broadening and peak shift at 1332 keV of less than 0.2 keV. Doppler broadening of lines due to decay in flight of nearly all reaction products led to final line widths on the order of 10 keV for γ rays of energy 1 MeV.

Particles of atomic number $Z\geq 3$ were detected in a gas proportional ΔE, solid state detector E telescope modeled after a design reported by Markham *et al.*[29] The proportional section, using a resistive Nichrome wire of 10 μm diameter, permitted both a measurement of particle energy loss ΔE and of particle position along the wire, using the method of charge division. The counter subtended a solid angle of 19 msr and covered an angular range of 24.9° to 33.3° in the laboratory system. A permanent grid of 1 mm diameter steel wires spaced 4 mm apart provided a position calibration. It was possible to resolve Z groups up to Na and occasionally Mg (Fig. 3) and to determine position within 1.5 mm for count rates up to 10 kcps.

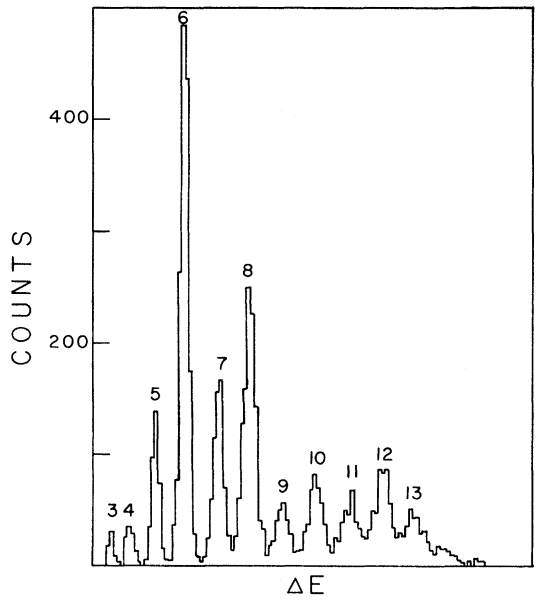

FIG. 3. ΔE spectrum in the gas proportional counter for the DIC region. The atomic number Z is shown for each group.

TABLE II. Positions of the heavy ion, Ge(Li), and NaI(Tl) (when used) detectors in various runs studying HI-γ coincidences in DIC of 100 MeV $^{16}O+^{27}Al$. The beam axis is taken as the x axis direction, and the z axis is taken along $\vec{k}_i \times \vec{k}_f$, where $\vec{k}_i$ and $\vec{k}_f$ are initial and final heavy ion directions, respectively.

Detector	Run 1		Run 2		Run 3		Run 4	
	θ	ϕ	θ	ϕ	θ	ϕ	θ	ϕ
HI detector	90°	24.9°−33.3°	90°	24.9°−33.3°	90°	24.9°−33.3°	90°	24.9°−33.3°
Ge(Li)	90°	270°	180°		90°	315°	180°	
NaI(Tl) No. 1					90°	135°	45°	180°
NaI(Tl) No. 2					90°	225°	45°	0°
NaI(Tl) No. 3					45°	0°	90°	315°

The multiplicity distribution information was obtained by detecting γ rays, in coincidence with particles, in an array of three 7.6×7.6 cm ϕ NaI(Tl) detectors placed at various positions (see Table II) around the target at a distance of 16 cm from the target. A graded absorber consisting of disks of 3 mm thick Pb and 3 mm thick Cu was placed in front of each detector with the lead facing the target to reduce the energy dependence of the total efficiency of the NaI(Tl) detectors. Ideally, for such multiplicity measurements, the total efficiency in the NaI(Tl) detectors should be independent of γ-ray energy. In practice the efficiency exhibits a small energy dependence after addition of absorbers, and in the present case it exhibited a rapid decrease for energies below 250 keV. However, this should not affect the results seriously, as most γ rays emitted by the nuclei in question (*s-d* shell) have $E_\gamma > 350$ keV.

The positions of the Ge(Li) detector were chosen to obtain information on particle-γ correlations that could be interpreted easily in terms of alignment of the nuclear spins. As the γ-ray transitions studied are mostly either $M1$ or $E2$, a convenient set of angles is perpendicular to the reaction plane, and in the reaction plane at 90° to the beam axis. Data were also taken with the Ge(Li) detector at 45° to the beam axis in the reaction plane. The NaI(Tl) detectors were positioned to average over the particle-γ correlations. The angles (θ,ϕ) chosen for the γ detectors in the various experiments are listed in Table II.

The data were stored on line by the BNL Sigma-7 computer system. The following signals were recorded: energy loss, residual energy, and position from the particle detector, pulse heights from all γ ray detectors, and the particle-γ ray time-of-arrival difference for the Ge(Li) detector. These time-of-arrival difference signals for the NaI(Tl) detectors were monitored in an off-line multichannel analyzer and occasionally collected on-line to determine the true-to-random ratio for the NaI(Tl)-particle coincident events. All particle-γ ray coincidences were recorded; particle singles spectra were also recorded to allow later normalization of the coincidence results.

B. Description of spectra measured

For later use, the following terms are defined. "Singles Z spectra" refers to particle energy spectra for a given Z for all events observed in the particle detector. "Ge(Li) i-fold spectra" refers to γ-ray energy spectra from the Ge(Li) detector with the requirement of detection of a coincident heavy ion of a specified Z and range of inelasticity and detection of at least i coincident γ rays in the multiplicity array. Thus, a "Ge(Li) 0-fold spectrum" is a high resolution γ ray energy spectrum for particle-γ coincident events ignoring the information in the multiplicity array. The energy distribution of the observed γ rays was taken in order to extract yields for specific transitions. "NaI(Tl) i-fold spectrum" refers to a particle energy spectrum for a given Z with the requirement of detection of at least i coincident γ rays in the multiplicity array. In this case, the energy distribution of the heavy ion was taken in order to extract information on the mean and variance of the γ-ray multiplicity as a function of particle Z and reaction inelasticity.

Singles Z spectra were extracted for each Z group for $5 \leq Z \leq 11$. For use with the Ge(Li) i-fold spectra they were divided into 10 MeV wide Q bins (see below) and integrated. For use with the NaI(Tl) i-fold spectra they were transformed to an axis linear, in 1 MeV steps, to the reaction Q value.

Ge(Li) i-fold spectra were collected for each Z group and for "bins" 10 MeV wide in reaction Q value. Corrections were made for energy loss of the beam through half the target and for detected heavy

ions through the gas, window, and half the target.[30] The limits of the Q value bins were computed using two-body kinematics and the heavy-ion position information. The mass of a given heavy ion was taken as that of the most abundant isotope of that Z (see Fig. 1). Only Z cuts and multiplicity-fold cuts were made for the generation of the NaI(Tl) i-fold spectra.

For the Ge(Li)-particle coincidence results Ge(Li) energy spectra were collected corresponding to 7 Z cuts ($5 \leq Z \leq 11$), 2 time-to-amplitude converter (TAC) cuts (prompt and delayed transitions), 6 Q-bin cuts (0—10 MeV to >50 MeV), and 4 NaI(Tl) fold levels (0, 1, 2, and 3 fold), where here n fold means events in which at least n NaI(Tl) detectors register a coincidence. For the NaI(Tl)-particle coincidence results, particle energy spectra were collected corresponding to 7 Z cuts and 1, 2, and 3-fold γ-ray coincidences.

From the Ge(Li) coincidence energy spectra, transitions in residual nuclei were identified and their yields extracted for the Z and Q-bin cuts employed. The yield for a transition is defined as $Y=N/(N_s\epsilon_\gamma f)$, where N is the number of coincident events, N_s is the number of particle singles counts for the appropriate Z and Q bin, ϵ_γ is the full-energy peak efficiency of the Ge(Li) for the transition and experimental geometry in question, and $f=e^{-t_1 \ln 2/T_{1/2}}-e^{-t_2 \ln 2/T_{1/2}}$ is the fraction of nuclei which decay within the given TAC gates. For these, t_1 and t_2 are the start and stop times, and $T_{1/2}$ is the level half-life. For prompt transitions, $f=1$; for the few observed delayed transitions, $f \leq 1$. For example, for the 197 keV, 87 ns $\frac{5}{2}^+ - \frac{1}{2}^+$ transition in ^{19}F, $f=0.8$ for the 200 ns TAC range used.

The NaI(Tl) i-fold spectra were normalized by dividing, Q bin by Q bin, by the number of singles counts for a given Z. To estimate the error introduced by not correcting the singles Q value cuts for angle dependence and instead using only one central angle, a brief event-tape record of telescope-only parameters was sorted using the same Z, Q bin, and angle cuts as for the Ge(Li) i-fold spectra. Particle energy spectra were collected for each Q bin and angle bin for each Z. It was found that counts from angle bins larger and smaller in θ than the central bin compensated one another, leading to systematic errors of at most 5% in the numbers of singles counts.

C. Extraction of γ multiplicities

The NaI(Tl)-fold spectra were analyzed using the R method described by Hagemann *et al.*[31] to produce values of the mean multiplicity, $\langle M_\gamma \rangle$, and the variance of the distribution, $\sigma_M{}^2=\langle (M_\gamma - \langle M_\gamma \rangle)^2 \rangle$ as a function of Q value and coincident Z. These can be obtained from the measured quantities $R_i=(i \text{ fold counts})/(0 \text{ fold counts})$ and the average total efficiency Ω of the NaI(Tl) detectors, using the relationships[31]

$$\langle M_\gamma \rangle \Omega = R_1 + \tfrac{1}{2}R_2 + \tfrac{1}{3}R_3 + \cdots , \tag{1a}$$

$$\langle M_\gamma (M_\gamma - 1) \rangle \Omega^2 = R_2 + R_3 + \cdots , \tag{1b}$$

$$\langle M_\gamma (M_\gamma - 1)(M_\gamma - 2) \rangle \Omega^3 = R_3 + \cdots . \tag{1c}$$

As only three NaI(Tl) detectors were used in the present experiments, the values for $\langle M_\gamma \rangle$ and σ_M extracted necessarily suffer from truncation errors due to the need to terminate all series at R_3. The value $\langle M_\gamma \rangle$ is sufficiently low, $2 \leq \langle M_\gamma \rangle \leq 4$, that the error introduced is small: Systematic errors of 1—2% in $\langle M_\gamma \rangle$ and $\sim 10\%$ in σ_M may result from the truncation. Fast neutron events detected in the NaI(Tl) counters were accepted in the time windows set, but from the low neutron multiplicity expected (~ 1) and low detection efficiency for neutrons compared to γ rays ($\sim 10\%$),[32] less than a 5% error in the values of R_i used to calculate $\langle M_\gamma \rangle$ and σ_M results.

For the particle-Ge(Li) coincidence data only the 0-fold and 1-fold spectra had sufficient counts to allow extraction of the peak yields. The expansion for $\langle M_\gamma \rangle$ is thus truncated at R_1, which leads to larger errors than for the particle-NaI(Tl) coincident data. However, the errors due to counting statistics were of equal or greater importance than these systematic effects in all cases in which it was possible to extract a yield. The errors shown later represent the statistical error only.

Two other sources of error should be mentioned. One is the uncertainty in efficiency of the Ge(Li) detector, and the second arises from mistaken 2- or 3-fold coincidences among the NaI(Tl) detectors that are due to detector-to-detector Compton scattering. The Ge(Li) efficiency has error contributions from counting statistics (1—3%), source calibration accuracy (3%), and peak extraction accuracy (estimated $\sim 5-10\%$) leading to an absolute error of $\sim 10\%$ for gamma ray energies below 3.5 MeV. Above that energy the efficiency was extrapolated relying on published curves for Ge(Li) detectors of about the same size and distance from the target.[33] This uncertainty principally affects the values of the yields for the $2^+ - 0^+$, 4439 keV transition in ^{12}C and the $3^- - 0^+$, 6130 keV transition in ^{16}O. A check on these yields was made by also

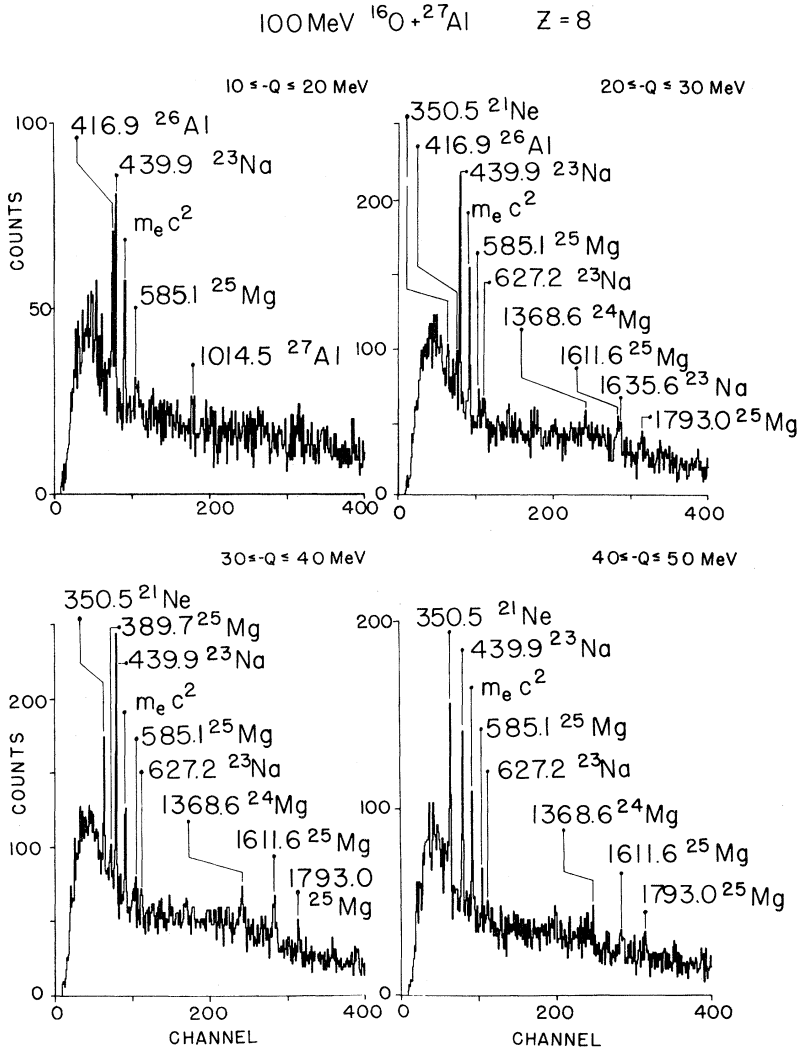

FIG. 4. Coincident Ge(Li) gamma-ray energy spectrum for HI-Ge(Li) coincidences for specific Q bins.

extracting the single and double escape peak yields and correcting for the single and double escape efficiencies, which have different extrapolations than the full-energy peak efficiency. Agreement of the results to within 20% was achieved. Mistaken coincidences between NaI(Tl) detectors due to detector-detector Compton scattering were checked by counting coincidences from monochromatic ^{137}Cs and ^{54}Mn sources, as well as by checking the multiplicity determination accuracy using a ^{60}Co source. The small number of mistaken coincidences observed for the monochromatic sources indicated a negligible ($< 1\%$) contribution to the 2 and higher-fold counting rates.

III. RESULTS

A. Particle-Ge(Li)-0 fold coincidence measurement

Samples of coincident energy spectra are shown in Fig. 4. One immediately notes the relative paucity of transitions observed, in contrast to the results of studies of fusion reactions, notably for the same system (see Fig. 1 of Dauk *et al.*[25]).

For the observed γ-ray transitions, yield curves as a function of Q value are shown in Figs. 5 and 6 for each Z group analyzed. Open circles denote results with the Ge(Li) detector perpendicular to the reac-

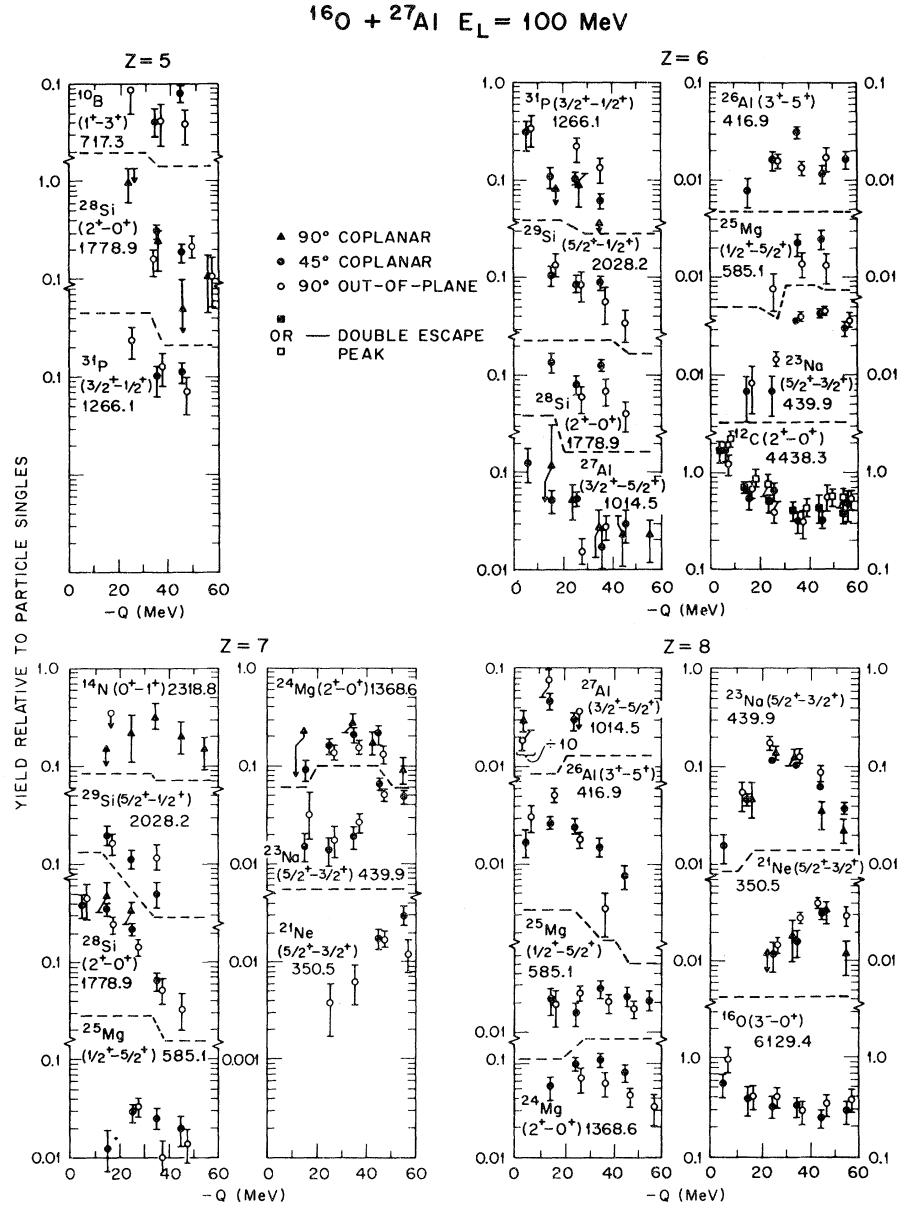

FIG. 5. Yields relative to HI particle singles for several transitions in coincidence with $Z=5$ through $Z=8$. Yields are given for 10 MeV wide bins in reaction Q value, calculated using two body kinematics.

tion plane, closed circles denote results with the Ge(Li) detector in the reaction plane at 45° to the beam axis, and triangles denote results with the Ge(Li) detector in the reaction plane at 90° to the beam axis. Most yields exhibit a broad, smooth bumplike shape with a FWHM often exceeding 20 MeV or more, not unlike the particle singles yields, with a peak value in the range of $-Q=25-40$ MeV. The position of the peak shifts to more negative Q values with increasing numbers of light particles emitted in the final stage.

All peaks in the coincident Ge(Li) energy spectra could be assigned either to the detector projectilelike fragment or to the targetlike fragment less one or more light particles. In several cases the Doppler shift was used in deciding the origin of the observed γ ray. It was found that most of the observed transitions were between low-lying states along the yrast line in the heavy partner, although a few cases of sidefeeding, notably from low-spin states, and a few

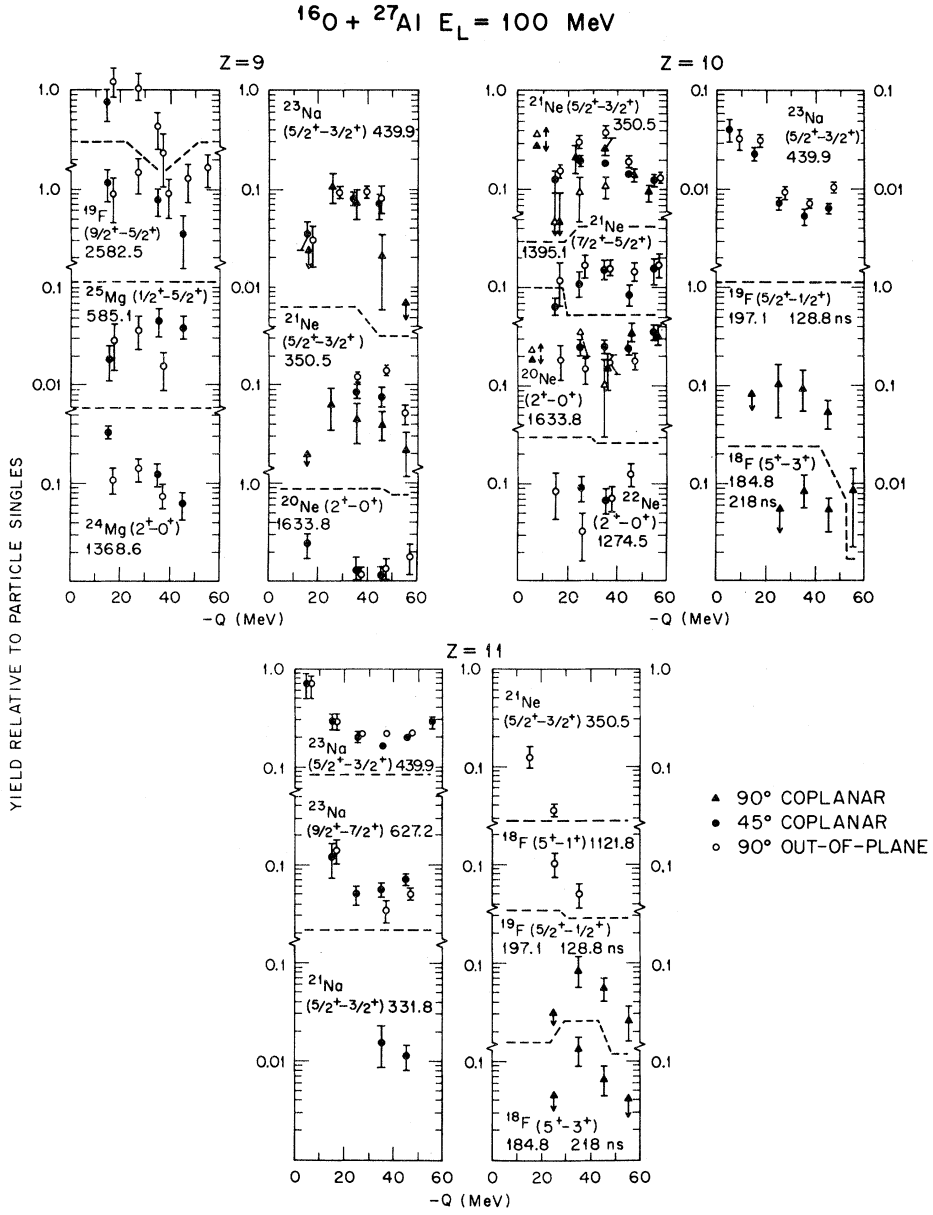

FIG. 6. Yields relative to HI particle singles for several transitions in coincidence with $Z=9$ through $Z=11$. Yields are given for 10 MeV wide bins in reaction Q value, calculated using two body kinematics.

projectilelike fragment transitions, e.g., the 2^+-0^+ 4439 keV transition in ^{12}C and the 3^--0^+ 6130 keV transition in ^{16}O were also observed.

From these yields the summed radiative yield was extracted. This is the fraction of detected ions in which at least one γ transition was observed, correcting for detector efficiency and solid angle. This determination is complicated by isomerism, angular correlation effects, and hard-to-detect high energy statistical γ-ray decay directly to the ground state. In the present work, the yield relative to particle singles is measured, and the desired sum not only extends over all exclusive transitions in one nucleus, but also over all possible heavy (light) fragments seen in coincidence with a specific Z in obtaining the total radiative strength for the targetlike (projectilelike) fragments. For the light fragments, only transitions in the various isotopes of the detected Z are included. If all primary fragments produced deexcited ultimately by γ emission, and all ground-state transitions had sufficient intensity to be observed, then a value of 1 for the summed ra-

TABLE III. Summed radiative yields for deeply inelastic collisions of 100 MeV $^{16}O+^{21}Al$. Yields for the detected light fragment are given first for each Z; undetected heavy fragment yields are given second.

	Fragment			$-Q$ (MeV)			
Z	Light (L) or Heavy (H)	0–10	10–20	20–30	30–40	40–50	>50
5	L				0.18	0.16	
	H			0.94	0.42	0.30	0.10
6	L	~1.0	0.53	0.64	0.31	0.32	0.48
	H	0.44	0.51	0.35	0.39	0.12	0.06
7	L	~1.0	0.17	0.29	0.26	0.20	0.14
	H	0.39	0.67	0.55	0.37	0.32	0.13
8	L	0.72	0.38	0.32	0.31	0.24	0.29
	H	0.36	0.22	0.37	0.39	0.27	0.07
9	L		0.62	0.65	0.52	0.29	0.07
	H		0.63	0.26	0.47	0.38	0.08
10	L			0.54	0.47	0.43	0.45
	H	0.39	0.47	0.63	0.39	0.19	0.21
11	L	0.68	0.29	0.37	0.40	0.40	0.27
	H			0.07	0.22	0.12	0.07

diative strength relative to particle singles would be expected for both the light and heavy fragments.

Summed radiative yields, averaged over the 90°-in-plane and out-of-plane geometries, are given in Table III. The values are generally in the range of 30–70%. The values are quite small for the most inelastic Q bin, $-Q > 50$ MeV. (A simple explanation of this last decrease might be contamination of the particle singles by fusion events, either with ^{27}Al, which have a much larger cross section than the deeply inelastic events at this energy, or with light target impurities.) Only in the quasielastic region are the strengths around unity.

B. Particle-NaI(Tl) γ multiplicity

The values for $\langle M_\gamma \rangle$ and σ_M for the various Z groups are shown in Figs. 7 and 8 as a function of

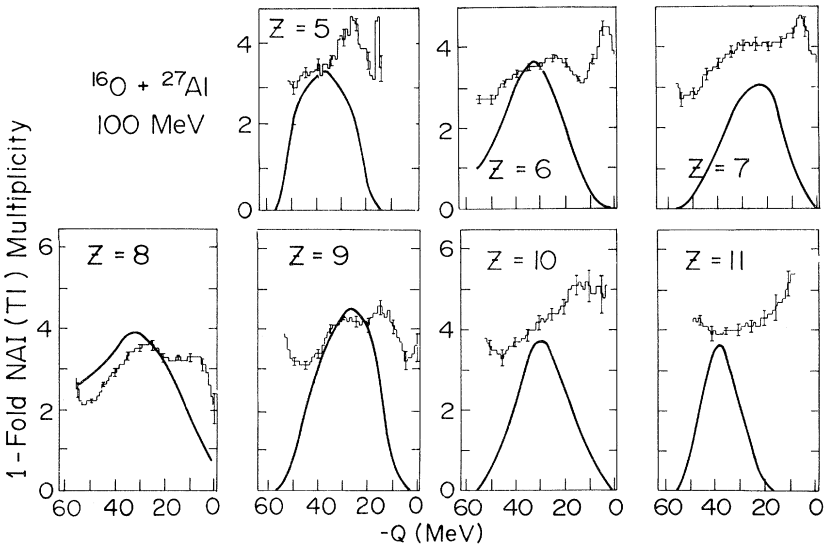

FIG. 7. Average multiplicity of gamma rays, determined from the HI-NaI(Tl) coincidence measurements, as a function of reaction inelasticity (1 MeV-wide bins in Q value) for elements $5 \leq Z \leq 11$ for the reaction 100 MeV $^{16}O+^{27}Al$. The rise at the most negative Q values is probably due to contamination of the Z groups selected in the HI ΔE-E maps with contributions from low energy, low ΔE evaporation residues that have a larger average gamma ray multiplicity. The fully drawn curves show the shape of the corresponding HI singles spectrum as a function of Q value.

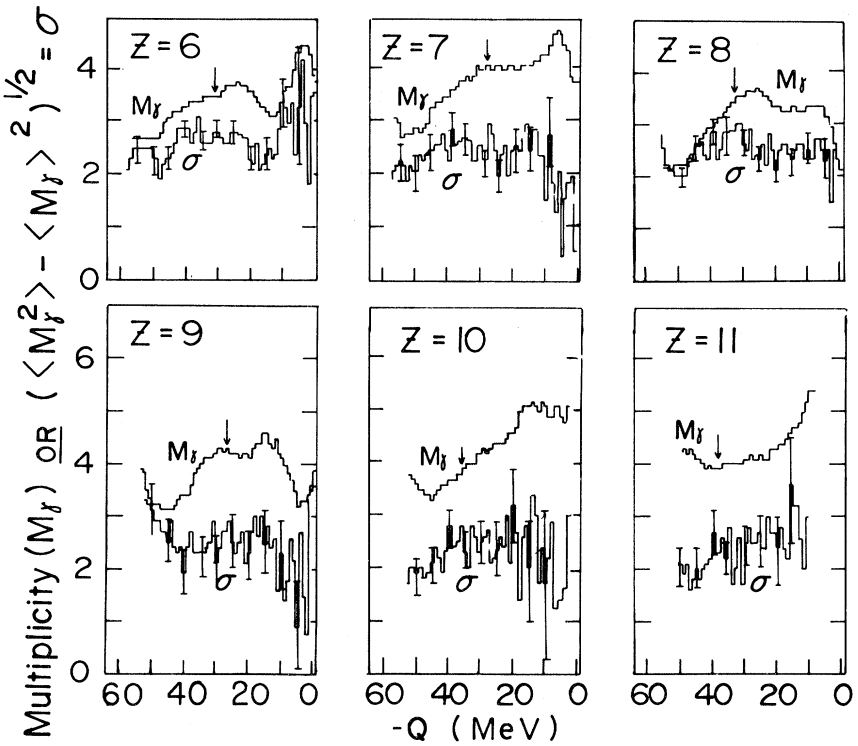

FIG. 8. Average multiplicity of gamma rays, $\langle M_\gamma \rangle$, and standard deviation, σ, of the multiplicity distribution as a function of inelasticity (1 MeV-wide bins in Q value) for the elements $6 \leq Z \leq 11$ produced in DIC. The arrow denotes the peak in the corresponding HI singles yield.

the reaction Q value. The shape of the particle singles spectrum is shown schematically in Fig. 7. The arrow in Fig. 8 indicates the position of maximum cross section of the corresponding particle singles group. Generally, $\langle M_\gamma \rangle$ has low values, decreasing almost monotonically with increasing inelasticity throughout most of the deeply inelastic region. The quasielastic region exhibits larger values of $\langle M_\gamma \rangle$ than does the DIC region, in contrast to other measurements involving heavier targets.[34,35] (However, the error bars are large for $Z=5$, 10, and 11, due to small particle singles yields in this region.) The appearance of the initial decrease of $\langle M_\gamma \rangle$ near $-Q=8-10$ MeV, the particle emission threshold, indicates the importance of particle emission. $\langle M_\gamma \rangle$ is relatively constant in the DIC region relative to the Z of the detected particle. The σ_M values observed of 2—3 indicate that the multiplicity distributions are quite wide (relative to their mean), spanning several units of multiplicity from below one to above seven.

A crude estimate of the average γ-ray energy $\langle E_\gamma \rangle$ was obtained from the NaI(Tl) detectors by comparing measured mean energies of pulse height distributions from the decay of radioactive sources with the actual mean energy computed from the known level scheme. Such an estimate leads only to a lower limit of $\langle E_\gamma \rangle$ when applied to spectra from a reaction. Yet, when combined with a value for $\langle M_\gamma \rangle$, a useful estimate of the total energy emitted in γ decay is obtained. Values of $\langle E_\gamma \rangle$, $\langle M_\gamma \rangle$, and $\bar{E}=\langle E_\gamma \rangle \cdot \langle M_\gamma \rangle$ for each Z group, are given in Table IV. (Such a relationship for $\bar{E}$ assumes the E_γ and M_γ distributions are uncorrelated.) The errors in $\langle E_\gamma \rangle$ are about ± 200 keV.

C. Particle-Ge(Li) coincidence NaI(Tl)-γ multiplicity

Shown in Fig. 9 are the values of $\langle M_\gamma \rangle$ for specific transitions seen in coincidence with a given Z and for a given range of inelasticity (10 MeV Q bins). Poor statistics in the Ge(Li)-2 and higherfold coincidence spectra necessitated terminating the series in Eq. (1) at R_1 [with M_γ replaced by $(M_\gamma - 1)$], leading to an underestimate of the actual value of $\langle M_\gamma \rangle$ for the transitions shown. In contrast to the values of $\langle M_\gamma \rangle$ extracted from the particle-NaI(Tl)-i-fold results, the values of $\langle M_\gamma \rangle$ in these cases range between 3 and 10, albeit with large error bars.

TABLE IV. Estimated average gamma ray energies $\langle E_\gamma \rangle$ determined from the NaI(Tl) energy spectra in coincidence with various projectilelike fragments from DIC of 100 MeV $^{16}O+^{27}Al$. Also included are the mean multiplicity $\langle M_\gamma \rangle$ for each Q bin and the product $\bar{E}=\langle E_\gamma \rangle \cdot \langle M_\gamma \rangle$ which is the mean energy carried off by gamma emission if the E_γ and M_γ distributions are uncorrelated. All energies are in MeV.

		$-Q$ (MeV)					
Z		0–10	10–20	20–30	30–40	40–50	>50
5	$\langle E_\gamma \rangle$		2.3	2.3	2.3	2.3	1.7
	$\langle M_\gamma \rangle$		5.4	4.3	3.8	3.4	3.3
	$\bar{E}$		12.4	10.0	8.8	7.8	5.6
6	$\langle E_\gamma \rangle$	2.4	2.5	2.5	2.5	2.5	2.3
	$\langle M_\gamma \rangle$	4.1	3.3	3.7	3.5	3.1	2.5
	$\bar{E}$	10.1	8.2	9.2	8.5	7.6	5.7
7	$\langle E_\gamma \rangle$		2.6	2.6	2.6	2.5	2.2
	$\langle M_\gamma \rangle$		4.2	4.1	3.9	3.3	2.3
	$\bar{E}$		10.8	10.4	9.9	8.2	5.2
8	$\langle E_\gamma \rangle$	2.8	2.7	2.6	2.5	2.6	2.4
	$\langle M_\gamma \rangle$	2.9	3.2	3.5	3.3	2.6	1.6
	$\bar{E}$	8.2	8.9	9.1	8.4	6.6	3.9
9	$\langle E_\gamma \rangle$		2.2	2.1	2.1	2.1	2.1
	$\langle M_\gamma \rangle$		4.4	4.2	4.0	3.2	1.8
	$\bar{E}$		9.8	8.9	8.3	6.8	3.7
10	$\langle E_\gamma \rangle$		2.2	2.1	2.1	2.1	2.1
	$\langle M_\gamma \rangle$		5.1	4.4	3.9	3.5	1.6
	$\bar{E}$		11.1	9.1	8.1	7.3	3.3
11	$\langle E_\gamma \rangle$		2.2	2.3	2.3	2.2	2.2
	$\langle M_\gamma \rangle$		4.8	4.2	4.0	4.1	1.0
	$\bar{E}$		10.5	9.5	9.1	9.2	2.2

D. Yields as a function of geometry: alignment of fragment spins

The variation of the yield for a specific transition (seen in coincidence with a deeply-inelastic scattered fragment) on the angular position of the γ ray detector depends on the degree of spin alignment of the state emitting the γ ray. In the present experiment, the ratios of the yields for the 90°-in-plane and out-of-plane geometries and for the 45°-in-plane and out-of-plane geometries were extracted for several transitions. The resulting anisotropies for the second case, $A=W(90°,315°)/\ W(180°,\phi)$, or $W(90°)/W(180°)$, where $W(\theta,\phi)$ is the yield for a given Ge(Li) detector position, are shown in Fig. 10 as a function of inelasticity and Z of the coincident particle. (See Table II for the coordinate system used.) Anisotropies different from unity are observed for many transitions, with values greater than one for most quadrupole transitions and less than one for dipole transitions. This is expected for states with spin aligned perpendicular to the reaction plane. The anisotropy expected for transitions of mixed multipolarity, such as $E2$-$M1$ transitions, from aligned states is greater or less than one depending on the mixing ratio.

To determine whether the measured anisotropies were near those expected for transitions from states with spin with maximum *polarization* perpendicular to the reaction plane, as expected in a classical grazing picture of deeply inelastic reactions, computations were made of the anisotropy expected for several transitions using the particle-gamma angular correlation formalism given by Rybicki, Tamura, and Satchler.[36]

The angular correlation can be written

$$W(\theta_\gamma,\phi_\gamma)=\sum_{\substack{K,Q \\ \text{even}}} A_{KQ} Q_K Y_{KQ}(\theta_\gamma,\phi_\gamma) ,$$

where $Y_{KQ}(\theta_\gamma,\phi_\gamma)$ are spherical harmonics. The

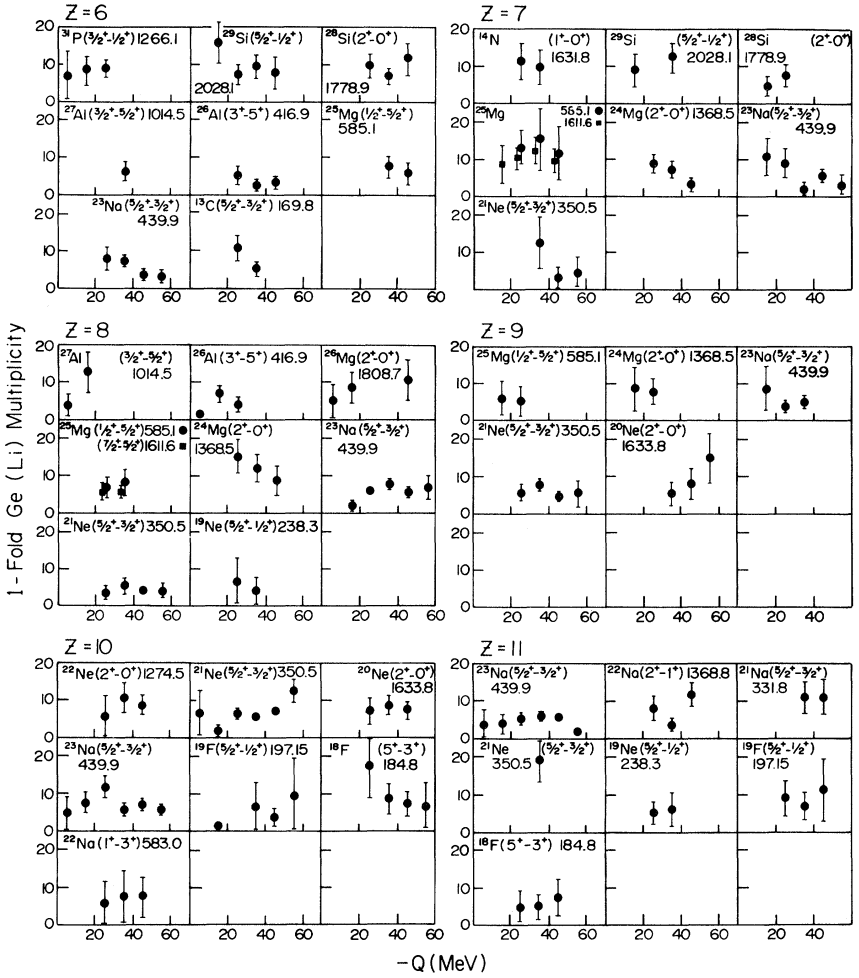

FIG. 9. Average multiplicity of gamma rays in coincidence with various discrete gamma transitions detected in the Ge(Li) detector for elements $6 \leq Z \leq 11$ and 10 MeV wide bins in reaction Q value.

Q_K, geometric attenuation factors due to the finite solid angle subtended by the Ge(Li) detector, were obtained from the tables of Camp and Van Lehn.[37] Correlation coefficients, A_{KQ} are normalized such that $A_{00}=1$ and can be written

$$A_{KQ}=[4\pi(2J+1)/(2K+1)]^{1/2}\rho_{KQ}F_K G_K \ .$$

The F_K for mixed multipolarity are given by

$$F_K=[R_K(LLJ_iJ_f)+2\delta R_K(LL'J_iJ_f)+\delta^2 R_K(L'L'J_iJ_f)]/(1+\delta^2) \ ,$$

where the Rosenzweig coefficients R_K are tabulated by Rose and Brink,[38] and the $E2$-$M1$ mixing ratios δ were taken from the compilations of Endt and Van der Leun,[39] who follow the phase convention of Rose and Brink.[38] The G_K are γ-ray attenuation coefficients due to the hyperfine interaction between the strong magnetic dipole field created by atomic K-shell vacancies and the magnetic dipole moment of the excited nuclear state recoiling into vacuum. In the present experiment, the time for a recoiling nucleus to leave the target is about 0.01 ps. While most lifetimes considered are about 1 ps, they are still short compared to the time required to significantly dealign the nuclear spin, and $G_K=1.0$ was used in the calculations. Two exceptions were made, however; they were the ^{21}Ne $(\frac{5}{2}^+ - \frac{3}{2}^+)$

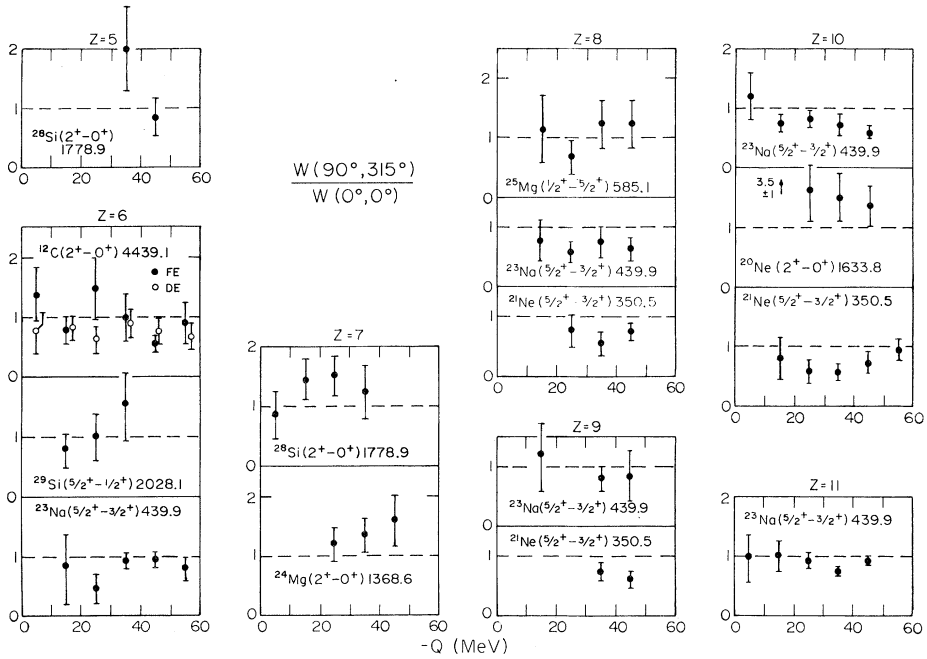

FIG. 10. In-plane versus out-of-plane anisotropies $W(90°,315°)/W(180°,0°)$ measured for various discrete gamma transitions in coincidence with the elements noted as a function of reaction inelasticity. The dashed lines indicate isotropic behavior of the particle gamma correlation.

350.5 keV transition with $t_{1/2}=20\pm3$ ps and the ^{24}Mg $(2^+\rightarrow 0^+)$ 1368.8 keV transition with $t_{1/2}=1.75$ ps. Calculations made for G_2 and G_4 not unity in these cases were found not to change significantly the computed anisotropy, as seen in Table V. (Note $G_0=1$ for all cases.)

The ρ_{KQ} are statistical tensors, written here in terms of $3J$ symbols.

$$\rho_{KQ}=(2K+1)^{1/2}\sum_{MM'} T_M T^*_{M'}(-)^{J-M'-Q}\begin{pmatrix} J & J & K \\ M & -M' & -Q \end{pmatrix},$$

where $T_M T^*_{M'}$ is an element of the density matrix. T_M is the complex amplitude for populating a given level of interest of spin J in magnetic substate M. Writing $T_M=|T_M|e^{-i\delta_M}$ and noting that for the present measurement one is interested in examining ratios of $W(\theta,\phi)$'s and not the cross section $d^2\sigma/d\Omega_p\, d\Omega_\gamma$, the normalization of the T_M's has been taken as

$$\sum_M |T_M|^2=1 .$$

Computed anisotropies $W(90°,315°)/W(180°,\phi)$, assuming complete alignment and polarization $(M_Z=J)$, are given in Table V for several transitions for which measured values could be obtained. For comparison, in a few cases, the computed anisotropies for the case of incomplete polarization, assuming a Gaussian distribution of the M-state population.

$$P(M)\equiv T_M T^*_{M'}\sim\exp[-(J-M_Z)^2/\sigma^2]\delta_{MM'} ,$$

$M\geq 0$, are also given, a similar parametrization as that in Puchta *et al.*[17]

IV. DISCUSSION

A. Yields, summed radiative strengths, and statistical model calculations

The final channels seen in this reaction are those expected for a primary deeply inelastic reaction

TABLE V. In-plane versus out-of-plane anisotropies $W(90°)/W(180°)$ computed for various discrete lines observed in gamma deexcitation following DIC of 100 MeV $^{16}O+^{27}Al$. All values for fully aligned and polarized case ($T_J^2=1$) unless noted.

Transition	E_γ (keV)	τ (ps)	δ	G_2	G_4	$\frac{W(90°,315°)}{W(180°,0°)}$
$^{21}Ne(\frac{5}{2}^+-\frac{3}{2}^+)$	350.5	20 ± 3	+0.030	1	1	0.465
				0.83	0.44	0.527[a]
				0.86	0.54	0.516[b]
$^{23}Na(\frac{5}{2}^+-\frac{3}{2}^+)$	439.9	1.60 ±0.08	−0.057	1	1	0.618
$^{31}P(\frac{3}{2}^+-\frac{1}{2}^+)$	1266.1	0.735±0.5	+ 0.29	1	1	0.310
						0.392[c]
$^{27}Al(\frac{3}{2}^+-\frac{5}{2}^+)$	1014.5	1.9 ± .2	+ 0.34	1	1	1.445
$^{12}C(2^+-0^+)$	4439.1	<1		1	1	44.9
$^{24}Mg(2^+-0^+)$	1368.6	1.75 ± .08		0.76	0.20	3.005
$^{28}Si(2^+-0^+)$	1778.9	0.68 ± .03		1	1	44.9
						1.813 to 1.842[d]
						7.57 to 81.97[e]

[a] G_2, G_4 calculated "hard core" values for recoil into a vacuum.
[b] G_2, G_4 calculated for 10 MeV recoil energy of ^{21}Ne.
[c] Calculated assuming M substates such that $T_{3/2}^2=0.9$, $T_{1/2}^2=0.1$; for $T_{3/2}^2=0.6$, $T_{1/2}^2=0.4$, $W(90°,315°)/W(0°,0°)=0.78$.
[d] Calculated for a polarized 2^+-0^+ transition with a Gaussian distribution of M substates of width $\sigma=1/\sqrt{2}$; $T_2^2=0.721$, $T_1^2=0.265$, $T_0^2=0.0132$; the low value is for $\delta_2-\delta_0=3\pi/2$, the high is for $\delta_2-\delta_0=\pi/2$.
[e] Calculated for a completely aligned and completely unpolarized case, $T_2^2=T_{-2}^2=0.5$. The low value is for $\delta_2-\delta_{-2}=\pi$, the high is for $\delta_2-\delta_{-2}=0$.

which results in two excited nuclei which then emit one or more light particles during their deexcitation (see Figs. 5 and 6). Transitions corresponding to just two body final states—^{27}Al in coincidence with $Z=8$, ^{31}P in coincidence with $Z=6$, etc., exhibit strong yields, approaching 100%, in the quasieleastic region. They decrease rapidly in yield with increasing excitation beyond roughly twice particle-emission threshold and become quite difficult to identify in the Ge(Li) 0-fold γ spectra for the $20<-Q<30$ MeV and $30<-Q<40$ MeV bins, even though these Q bins have the best particle singles counting statistics. The yield falls rapidly for the most inelastic regions for all transitions, in many cases the summed observed yields from heavy fragments being as little as 10%.

1. *Carbon final channels*

Transitions in coincidence with carbon give an example of the shift of the yield curves centroids to regions of greater inelasticity with increasing particle emission. The $^{31}P(\frac{3}{2}^+-\frac{1}{2}^+)$ transition, which corresponds to no particle emission in coincidence with ^{12}C, is peaked in the first Q bin and decreases rapidly thereafter. However, it is still seen at large inelasticity $30<-Q<40$ MeV. This last result may be partly due to $1n$ decay of ^{32}P in coincidence with ^{11}C. The particle singles yield (from the TOF experiment)[27,28] for ^{11}C is 4% of that for ^{12}C, which would account for about half the observed yield. The few nucleon channels ^{28}Si and ^{29}Si are somewhat stronger than the 1α channel ^{27}Al, though the general shape of the yield curves is similar with greatest strength around $-Q=15-20$ MeV. The weaker channels involving multiple particle emission, such as $\alpha n(^{26}Al)$ and $\alpha p(^{26}Mg)$, are peaked around $-Q=35$ MeV, and the 2α channel ^{23}Na reaches a maximum for $-Q=45$ MeV. An alpha transfer reaction might be the means for producing ^{12}C from the projectile ^{16}O, though the fact that the ^{27}Al transition peaks so forward in $-Q$ would not rule out α emission from an excited ^{16}O.

The yields for the 4439 keV (2^+-0^+) transition in ^{12}C in coincidence with carbon shown in Fig. 5 are also seen to be less than unity. Correcting for the fraction of carbon particles that is ^{12}C, as deter-

mined from the TOF measurements (Fig. 1), it is found that these yields in the DIC region are about 50–70 %. This indicates there is a sizable chance for production of ^{12}C in the reaction in states, of which one could be the ground state, that do not decay via the 4439 keV, 2^+ state. [The yields for the 4439 keV transition in ^{12}C, as well as that for the 6130 keV ($3^- - 0^+$) transition in ^{16}O, are about 40% lower than those reported in Ref. 15. This is due to a correction of the Ge(Li) γ detection efficiency at high E_γ from that used in Ref. 15.]

2. *Oxygen final channels*

The yields for transitions seen in coincidence with oxygen provide the best illustration for the evidence of increasing inelasticity for increasing number of particles emitted. The ^{27}Al yield drops quickly from its peak in the quasielastic region; it is superseded by its neutron emission product, ^{26}Al, which peaks at $-Q=15$ MeV. The alpha channel, ^{23}Na, is next, peaking at $-Q=25$ MeV. The ^{25}Mg and ^{24}Mg channels involve either deuteron or *pn* emission with the location of the peak in the yield favoring the latter case. ^{21}Ne could be produced by (αpn) emission from ^{27}Al; it exhibits a peak in yield at the largest inelasticity, -50 MeV, observed for $Z=8$ coincidences.

Calculations of the statistical deexcitation of the targetlike fragment were carried out using the evaporation code JULIAN.[40] The decay of an excited ^{27}Al was calculated for an intial population at given, sharp spin values of $J=0$, 4, and 8 $\hbar$, for several excitation energies. The results are shown in Fig. 11 for the final nuclei for which γ-ray yields were measured. The experimental results have arbitrarily been multiplied by a factor of 3 and are given by the solid-line histogram. The dashed-line histogram shows the results of the calculation for $J=4$ averaged in 10 MeV wide bins of excitation energy.

The onsets of the yields for ^{26}Al, ^{23}Na, and the peak ($Q\simeq -40$ MeV) for ^{21}Ne are qualitatively reproduced by the calculations. This supports the interpretation that one of the dominant primary channels is inelastic excitation of ^{27}Al. That other reaction mechanisms are present is suggested partly by the relative broad yield, e.g., in the ^{23}Na channel, which could be partly populated via $^{16}O + {}^{27}Al \rightarrow {}^{23}Na + {}^{20}Ne \rightarrow {}^{23}Na + {}^{16}O + \alpha$ in a three-body process as suggested by Sasagase.[41]

The observed transitions all belong to nuclei having sizable cross sections in the statistical model

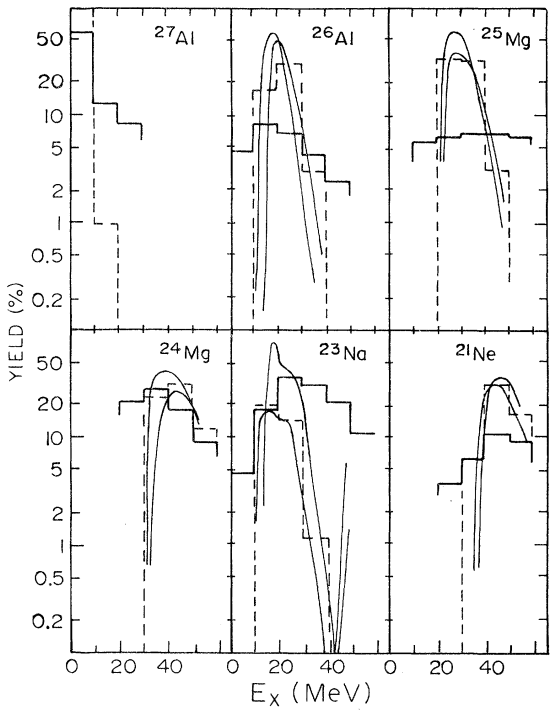

FIG. 11. Results of calculations using the statistical model code JULIAN for the yield of various targetlike fragments in coincidence with deeply inelastically scattered oxygen nuclei as a function of reaction inelasticity. The histograms are the present HI-Ge(Li) coincidence results (Fig. 5). The dotted histogram is a calculation with $J=4$ and averaged over 10 MeV wide bins. The other full drawn curves are for $J=0$ and $J=8$, with the latter always shifted to more negative Q values. The experimental strengths have been multiplied by 3 to account roughly for the missing radiative strength.

calculation. Nevertheless, two channels with sizeable cross sections in the calculation were not observed in the Ge(Li) spectrum: the ^{27}Al decaying to $^{22}Ne,\alpha p$, and to $^{26}Mg,p$. At the higher excitation energies the strength is predicted to be distributed over several channels, a fact which would partly explain the missing radiative yields. The probability for excitation of the targetlike fragment together with production of a "cold" projectilelike fragment can be studied for oxygen coincidences by examining the yield for the 6130 keV ($3^- - 0^+$) transition in ^{16}O. As shown in Fig. 5, this is less than unity. Correcting for the fraction of oxygen which is ^{16}O (Fig. 1) it is found that the yield is $\simeq 40-50$ %. This again indicates a sizable chance, ~ 55%, for the production of a cold ^{16}O in the reaction, as was the case for ^{12}C. It is noted, that in general, low yields are observed for transitions in projectilelike

nuclei and that a small number of different transitions in the projectilelike fragment is seen for all Z groups.

3. Summed radiative yields

The summed radiative yields are given in Table III as a function of Z and inelasticity. Generally low values are found. One does indeed expect summed radiative yields less than unity due to the direct population of ground states in the reaction. The unusual feature here is the magnitude of the loss of strength. For example, in a study of $^{16}O+^{27}Al$ fusion, Dauk *et al.*,[25] using a statistical model, estimated the direct population of ground states after particle evaporation from the fused nuclei and found it to be $\simeq 20\%$ at an excitation energy of 24 MeV and $<2\%$ at energies above 40 MeV. In contrast, a loss of strength greater than 50% is often observed in the present work. As opposed to heavy-ion induced fusion reactions, which transfer all of the initial orbital angular momentum to the spin of the compound nucleus and subsequently exhibit γ decay patterns that closely follow the yrast line, in deeply inelastic reactions only a fraction of the orbital angular momentum is transferred to intrinsic fragment spin ($\frac{2}{7}$ in the rolling limit). The primary population, being located farther from the yrast line than that in a fusion-evaporation reaction, might often undergo decay via a cascade of "statistical" γ transitions leading to the ground state, which, due to the fragmentation of strength, are not included in the measured summed radiative yield and thus would lead to an apparently low value of summed radiative strength.

B. NaI(Tl)-multiplicity discussion

For the decay of heavy nuclei ($A \geq 60$) produced in (HI, xn) reactions a linear relation between average angular momentum and γ-ray multiplicity has been demonstrated,[42] with the average spin and γ-ray multiplicity related by

$$\langle I \rangle = f_\gamma \cdot (\langle M_\gamma \rangle - M_s) + f_n x_n \ .$$

Here M_s is some number of statistical γ rays, often $E1$ in nature, which carry off little or no net angular momentum. The factor f_γ is characteristic of the cascades in the deexciting nucleus, being $2\hbar$ for stretched $E2$ cascades, while f_n and x_n are the corresponding factor for particle (neutron) evaporation and the number of neutrons emitted in producing the evaporation residue. For heavy systems f_n is typically $\sim 0.9\hbar$.[12]

In the present case it is important to treat the particle emission in interpreting the values of $\langle M_\gamma \rangle$. An attempt at a quantitative treatment for evaporation particles for light systems has been suggested by Mollenauer[43] and by the Heidelberg group[10] in discussing γ-ray multiplicities in fusion and deeply inelastic reactions, respectively. Mollenauer suggested correcting for particle emission by a term $(\partial I/\partial E_x)\cdot E_x$, which is the same method as above for neutron emission (at least for heavy systems), as the number of neutrons emitted depends linearly on E_x by ~ 1 neutron/10 MeV, and each removes approximately the same angular momentum. In his analysis Mollenauer used a value for $\partial I/\partial E_x = 3\hbar/16$ MeV. Then, the primary spin can be expressed

$$I_{\text{primary}} = f_\gamma \cdot (M_\gamma - M_s) + \partial I/\partial E_x \cdot (E_x - E_x^0) \ ,$$

where E_x^0 is an initial offset in excitation energy. In deeply inelastic collisions, choices for the two derivative coefficients are not immediately obvious because the entry points in the two fragments may be well away from the yrast line and thus the cascades may not admit a stretched $E2$ description. Values of f_γ ranging from 2 to $2.4\hbar$ have been used; the Heidelberg group has chosen the Mollenauer value for $\partial I/\partial E_x$ for their studies of $^{16}O+^{58}Ni$.[10]

Similar to other analyses of DIC γ-multiplicity data, we wish to compare our measured $\langle M_\gamma \rangle$ values to those obtained by assuming that the fragments stick together and undergo rigid rotation before separation as discussed by Tsang.[14] Assuming that the fragments have moments of inertia J_1 and J_2 and radii R_1 and R_2, one obtains

$$\Delta L = \frac{J_1 + J_2}{M_r (R_1 + R_2)^2 + J_1 + J_2} l_i \ ,$$

where ΔL is the total angular momentum transferred to intrinsic spin, l_i is the initial orbital angular momentum, and M_r is the reduced mass. We have estimated $\langle M_\gamma \rangle$ using the formula given above with choices of $f_\gamma = 1.5$ and 2 $\hbar$ and $(\partial I/\partial E_x)$ of $3\hbar/16$ MeV and $1.5\hbar/16$ MeV and with $E_x^0 = 8$ MeV and $M_s = 0$. One would expect the choice of $f_\gamma = 1.5\hbar$ to take better account of the numerous mixed $E2$-$M1$ transitions in s-d shell nuclei. The initial partial waves contributing to the deeply inelastic collisions are assumed to be the

same for all Q values and to be the grazing partial waves, $l_i = 31$ to 37 $\hbar$, which account for the measured deeply inelastic cross section in a sharp cutoff model. The results are shown in Fig. 12 together with the data for $Z=6$ to $Z=11$. The choice of $(\partial I/\partial E_x)$ of $1.5\hbar/16$ MeV appears to describe correctly the dependence of $\langle M_\gamma \rangle$ with E_x. This dependence is consistent with the results of Dayras *et al.*[44] for the ^{20}Ne+^{63}Cu system. However, either there is a change in f_γ from 2 to 1.5 $\hbar$ with increasing Z or the model is inappropriate. The observed $\langle M_\gamma \rangle$, being approximately constant, independent of Z, does not follow from the model in a simple way, and is probably not a result of such a large change in f_γ over this narrow range of residual nuclei, but rather probably that the sticking condition is not fulfilled for a large fraction of DI collisions.

The same model predicts the initial widths of the spin distributions in the two fragments to be quite small, $\sigma_L \sim 2\hbar$, ignoring angular momentum spreading due to light particle emission. However, due to the thermal fluctuations in the angular momentum transfer, for nuclei described as Fermi gases one expects a width of $\sigma_L \sim 0.5\langle \Delta L \rangle$ (Ref. 45) or about $4\hbar$ for equal sized fragments in the exit channel. This then leads to a value of $\sigma_M \sim 2-3$, in agreement with the data (see Fig. 8).

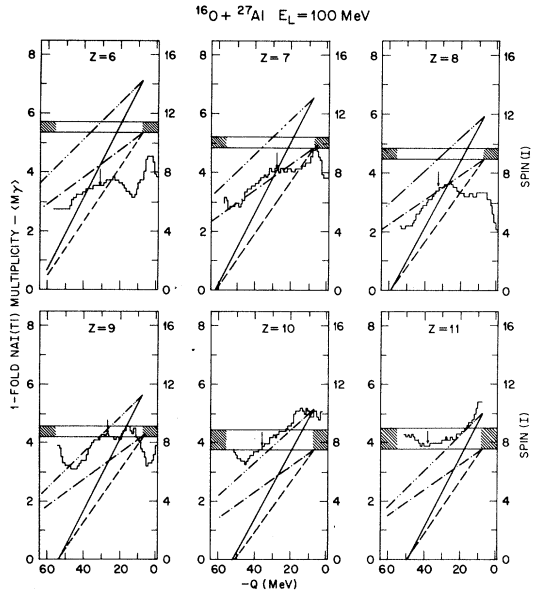

FIG. 12. Comparison of measured multiplicities (histograms) from the HI-NaI(Tl) results with the predictions of the sticking model of Tsang (Ref. 14.) The horizontal bands indicate the expected initial spin for a range of spherical ($\delta=0$) to deformed ($\delta=0.3$) final fragments. The solid (dashed) and dot-dot-dashed (dot-dashed) lines show the calculated $\langle M_\gamma \rangle$ for $f_\gamma = 1.5$ $\hbar$ ($2\hbar$) for the two choices of $(\partial I/\partial E_x) = 3\hbar/16$ MeV and $1.5\hbar/16$ MeV, respectively.

C. Discussion of Ge(Li) $\langle M_\gamma \rangle$ results

The multiplicities for specific channels are larger than the NaI(Tl) results, as might be expected from the low values found for summed radiative yields. When a channel includes at least one γ ray, as is required in the gating requirement used here, that the Ge(Li) fire, then it often includes several. Although both fragments in the final state can γ decay for all final pairs seen, only $1-2$ γ rays can be emitted by the light fragment, as higher excitation would lead to fragment breakup. Most of the observed multiplicity must arise from decay of the heavy fragment, which has the higher level density. For comparison to the values of $\langle M_\gamma \rangle$ given here, a survey was made of the number of γ rays emitted in the deexcitation of levels with $E_x \leq 8$ MeV using the level schemes and branching ratios given by Endt and Van der Leun.[39] Values between two and four γ rays emitted were found for all levels except the lowest, which require fewer γ rays to deexcite. Including an average of 1.5 statistical feeding γ rays for each fragment would give a total of $5-7$ γ, rays, which is generally somewhat above the values obtained from the particle-Ge(Li) multiplicity measurements.

Of particular interest are channels which include little or no light particle emission, such as ^{31}P, ^{29,28}Si, and ^{27}Al in coincidence with $Z=6$, 7, and 8, respectively. All these multiplicities have values of about ten, higher than the value $2 < \langle M_\gamma \rangle < 4$ obtained from the NaI(Tl) results. The large $\langle M_\gamma \rangle$ found after emission of one nucleon indicates that a considerable amount of angular momentum is present in the initial collision. Comparing these channels to those for which successively more particle emission is present, a slow decrease in multiplicity as more light particles are present in the final channel is indicated. This reflects the fact that the particles remove angular momentum, reducing the number of γ rays emitted in the next stage. $\langle M_\gamma \rangle$ for a specific transition is seen to exhibit little dependence on Q, except for a few transitions [e.g., ^{23}Na $(\frac{5}{2}^+ - \frac{3}{2}^+)$ in coincidence with $Z=8$], whereas the yield for the same transition may vary by two orders of magnitude over the same range in Q. As there is no change in the number of particles emitted for these individual transitions, except for

one or two neutrons from the projectilelike fragments, that flat behavior again points up the importance of excitation energy *and* angular momentum removal by particle emission.

A consistency check can be made on the radiative strength and multiplicity results by computing the total average multiplicity from the Ge(Li) i-fold coincidence results and comparing it with that extracted from the NaI(Tl) i-fold results. If one could observe all discrete transitions and measure their yields and multiplicities, one should reproduce the value from the NaI(Tl) results via

$$\langle M_\gamma \rangle_{\mathrm{Ge}} = \frac{\sum_i Y_i \langle M_\gamma \rangle_i}{\sum_j X_j + \sum_i Y_i} ,$$

where Y_i is the yield for transition i, X_j is the yield for nuclei not deexciting by γ-ray emission (e.g., nuclei produced in their ground states), $\langle M_\gamma \rangle_i$ is the mean multiplicity for the transition with yield Y_i, and the sum over i runs over the same set of exclusive transitions as does that for the summed radiative yield, being restricted to either the observed or unobserved heavy ion, and always using the lowest member of an inclusive set of transitions. Here $\sum_j X_j$ was taken as being $1-\sum_i Y_i$, which is true in the case of complete experimental knowledge but is an approximation here. The values obtained, for $6 \leq Z \leq 9$ and 10 MeV Q bins, for the unobserved fragment are shown together with the $\langle M_\gamma \rangle$ values from the NaI(Tl) results in Fig. 13. Fair agreement is obtained with the exception of the $-Q > 50$ MeV bin, in which case $\langle M_\gamma \rangle_{\mathrm{Ge}}$ is systematically below $\langle M_\gamma \rangle_{\mathrm{NaI}}$ (partly due to contamination from evaporation residues as noted earlier in Sec. III A). If the fraction $\sum_j X_j$, assumed here to have a multiplicity of zero, was composed of high energy-low multiplicity cascades, for which the present detection efficiency is poor due to the Ge(Li) response, the computed value of $\langle M_\gamma \rangle_{\mathrm{Ge}}$ would increase. Assuming this fraction $\sum_j X_j$ to have an average multiplicity of 1–2 yields values of $\langle M_\gamma \rangle_{\mathrm{Ge}}$ quite near those of $\langle M_\gamma \rangle_{\mathrm{NaI}}$. That the Ge(Li) 1-fold results produce values of $\langle M_\gamma \rangle$ for specific transitions larger than the average values found from the NaI-(Tl) i-fold results, indicates that there exists a large contribution from events with low (<2) γ-ray multiplicity in addition to the 30–50 % contribution to the yield from the events seen in the Ge(Li) i-fold spectra which have a relatively high ($M_\gamma \sim 5-9$) multiplicity. This also suggests that the actual spread in transferred angular momentum is large in order to yield both a sizable fraction of low and of high multiplicity events.

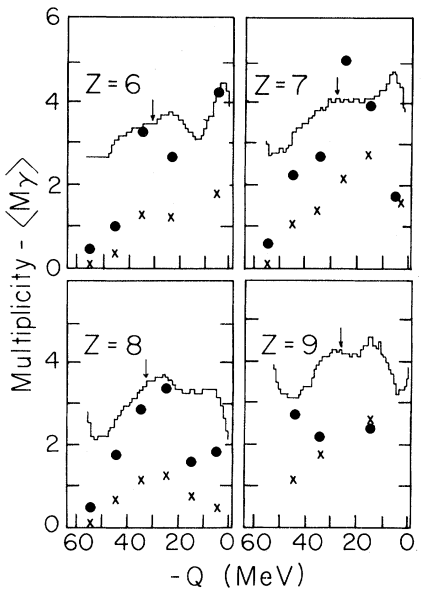

FIG. 13. Comparison for different Z groups and as a function of inelasticity of the average multiplicity of gamma rays determined from the HI-NaI(Tl) measurements (histograms) and from the HI-discrete line multiplicity and yield measurements (full circles). For reasons of counting statistics, the latter are averaged over 10 MeV wide bins in reaction Q value. [For comparison, the crosses mark the results of multiplying the summed radiative yield for discrete lines in coincidence with a given Z group and range of inelasticity by the mean multiplicity from the HI-NaI(Tl) results for the same Z group and inelasticity.]

The measured values of $\langle E_\gamma \rangle$ (see Sec. III B) are all above 2 MeV, much larger than the transition energies found for resolved transitions in the Ge(Li) spectra. In addition, the values for $\bar{E}$, the average total energy in γ decay, are concentrated between 8 and 10 MeV for all Z's and Q bins, with the exception of $-Q > 50$ MeV, in which case the drop in $\bar{E}$ is seen to be due principally to a corresponding drop in $\langle M_\gamma \rangle$. If states with spin values $> 6\hbar$ near the yrast line in the heavy partner were populated frequently, then due to the steepness of the yrast line in s-d shell nuclei a higher value for $\bar{E}$ would be expected due to the deexcitation of the heavy fragment alone.

D. Anisotropies

Comparison of the computed values for full polarization (alignment) of the in-plane versus out-of-

plane anisotropy of the coincident yield for discrete transitions, $A = W(90°,315°)/W(180°,0°)$, and the measured anisotropies shown in Fig. 10 indicates full polarization (alignment) values of the anisotropy are not reached in many cases, and a given transition may display values of A ranging from 1, consistent with an isotropic angular correlation and no alignment of the fragment spin, to a value consistent with full alignment, as the inelasticity of the reaction is varied. For example, the 439.9 keV $(\frac{5}{2}^+ - \frac{3}{2}^+)$ $E2$-$M1$ transition in ^{23}Na observed in coincidence with oxygen displays an isotropic correlation for $10 < -Q < 20$ MeV and displays an anisotropic correlation consistent with full alignment, with $A < 1.0$ as expected for this mixed transition, for $10 < -Q < 20$ MeV. The same transition seen in coincidence with carbon has a correlation that is anisotropic for $-Q < 30$ MeV and consistent with 1.0 for $30 < -Q < 50$ MeV. Dealigning effects are particle emission, various γ-ray deexcitation paths (spin sequences) from the primary states to the parent state of the observed transition, and generation of nonaligned components of angular momentum before separation of the intermediate dinuclear complex into primary fragments, as suggested by Moretto and Schmidt[46] and Vandenbosch.[47]

The observed anisotropy varies with the amount of particle emission. The anisotropies of the 1778.9 keV $(2^+ - 0^+)$ transition in ^{18}Si seen in coincidence with nitrogen and the 439.9 keV $(\frac{5}{2}^+ - \frac{3}{2}^+)$ transition in ^{23}Na seen in coincidence with neon all display anisotropies different from 1.0. In each of these cases one (or possibly, though improbably, two) neutrons have been emitted from the primary fragment. For the 1368.6 keV $(2^+ - 0^+)$ transition in ^{24}Mg seen in coincidence with nitrogen, the 350.5 keV $(\frac{5}{2}^+ - \frac{3}{2}^+)$ transition in ^{21}Ne seen in coincidence with fluorine, and the 350.5 keV $(\frac{5}{2}^+ - \frac{3}{2}^+)$ transition in ^{21}Ne seen in coincidence with oxygen, large anisotropies are observed for some range of inelasticity, although these cases correspond to at least emission of an α, and to αp emission for the last case. In a statistical picture these results would be expected if α's preferentially deexcite the high spin fraction of the states produced in the primary collision,[25,48] with the result that the larger l removed by the α's does not result in significant loss of spin alignment.

An alternative reason for the observed anisotropies for channels involving α emission is emission of an α during the initial stages of the reaction in a manner analogous to that suggested for incomplete fusion reactions,[49–51] followed by (deeply) inelastic scattering of the projectile and target "remnants." If such alpha emission were coplanar with the inelastic scattering, the orbital and fragment spin angular momentum would still be aligned perpendicular to the reaction plane. If no further particle emission dealigned the spins (corresponding here to seeing two heavy fragments whose masses and charges sum to those of the compound system less one α), a particle-γ angular correlation with A near or equal to the value for full alignment would be observed.

V. SUMMARY AND CONCLUSIONS

Deep inelastic collisions of 100 MeV ^{16}O with ^{27}Al were studied in a coincidence experiment between scattered fragments observed at an angle behind the grazing angle and with an array of both high resolution and low resolution γ detectors. The mean and variance of the γ-multiplicity distribution, the average energy of the γ decay, and the yields and anisotropies from specific transitions in the fragments were measured as a function of the inelasticity (or combined fragment internal energy) of the reaction products. The shapes of the observed yield curves for specific transitions, their maxima with respect to reaction inelasticity, and the relative populations of various heavy fragments seen in coincidence with a given projectilelike fragment indicate that statistical decay of a primary two-body final state is a correct description of the later stages of a deeply inelastic collision. Statistical evaporation calculations of the particle decay of selected targetlike fragments qualitatively describe the relative yields for specific final nuclei as a function of inelasticity. It was not possible, however, to obtain quantitatively the spin distribution of the primary fragments.

Strong yrast band γ decays of the targetlike fragments were generally found to be associated with large anisotropies in the γ-fragment correlations and were observed even for channels with several light particles emitted, including α particles. Thus, a large fraction of the deep-inelastic collision cross section can be characterized as producing fragments with modest angular momentum (consistent with sticking) and an alignment (or polarization) normal to the reaction plane.

The low measured summed radiative yield, yet high average γ-ray energy indicate that a large fraction of the fragments decay by a few high-energy (and thus difficult to detect) statistical gamma ray transitions. This part of the cross section (about 50% of the total) is thus characterized by low angu-

lar momentum transfer to the fragments.

A weakness of the experiment was the measurement of only the charge and not both charge and mass of the projectilelike fragment, so that some ambiguity in the identification of the reaction channel was introduced. Further ambiguities were introduced in the more mass symmetric exit channels, as particle evaporation from the projectile as well as targetlike fragment is significant. Nevertheless, one can conclude that for this system a large fraction of the cross section for deep-inelastic scattering is associated with low angular momentum transfer collisions, for scattering angles behind the grazing angle that are presumably a result of "negative-angle" scattering, for which one might assume that one predominantly reaches the sticking condition. This implies that the deep inelastic collisions may result from contributions from a broader band of partial waves than merely those of largest l close to the grazing partial wave. Measurement of the alignment for specific exit channels as a function of scattering angle and bombarding energy may be able to elucidate further the partial wave dependence of the cross section.

ACKNOWLEDGMENTS

The authors thank the tandem Van de Graaff staff and accelerator crew at Brookhaven National Laboratory for excellent operation during the performance of these experiments. Helpful conversations were had with Dr. L. Grodzins, Dr. J. Harris, Dr. I.-Y. Lee, Dr. R. Robinson, Dr. R. Dayras, and Dr. T. Døssing. Help during experiments and certain parts of the analysis was provided by Dr. C. Flaum and J. Karp and R. Ledoux. G.R.Y. acknowledges support from a National Science Foundation predoctral fellowship and a Chaim Weizmann postdoctoral fellowship during the course of this work and F.V. thanks the Danish Natural Science Research Council for support. This research was sponsored by the U. S. Department of Energy under Contract No. DE-AC02-76-ER03069.

---

*Present address: Physics Division, Oak Ridge National Laboratory, Oak Ridge, Tennessee 37830.

†Present address: Physics Department, Stanford University, Stanford, California 94305.

‡Present address: Physics Department, The University of Washington, Seattle, Washington 98195.

[1]P. Dyer, R. J. Puigh, R. Vandenbosch, T. D. Thomas, and M. S. Zisman, Phys. Rev. Lett. 39, 392 (1977).

[2]C. K. Gelbke, P. Braun-Munzinger, J. Barrette, B. Zeidman, M. J. Levine, A. Gamp, H. L. Harney, and Th. Walcher, Nucl. Phys. A269, 460 (1976).

[3]D. v. Harrach, P. Glässel, Y. Civelekoglu, R. Männer, and H. J. Specht, Phys. Rev. Lett. 42, 1729 (1979).

[4]B. Cauvin, R. C. Jared, P. Russo, R. P. Schmidt, R. Babinet, and L. G. Moretto, Nucl. Phys. A301, 511 (1978).

[5]J. Harris, T. M. Cormier, D. F. Geesaman, L. L. Lee, R. L. McGrath, and J. P. Wurm, Phys. Rev. Lett. 38, 1460 (1977).

[6]H. Ho, R. Albrecht, W. Dünnweber, G. Graw, S. G. Steadman, J. P. Wurm, D. Disdier, V. Rauch, and F. Scheibling, Z. Phys. A 283, 235 (1977).

[7]R. K. Bhowmik, E. C. Pollacco, N. E. Sanderson, J. B. A. England, and G. C. Morrison, Phys. Rev. Lett. 43, 619 (1979); C. K. Gelbke, M. Bini, C. Olmer, D. L. Hendrie, J. L. Laville, J. Mahoney, M. C. Mermaz, D. K. Scott, and H. H. Wieman, Phys. Lett. 71B, 83 (1977); A. Gamp, J. C. Jacmart, N. Poffé, H. Doubre, J. C. Roynette, and J. Wilczyński, *ibid.* 74B, 215 (1978).

[8]M. Berlanger, M. A. Deleplanque, C. Gerschel, F. Hanappe, M. Leblanc, J. F. Mayault, C. Ngô, D. Paya, N. Perrin, J. Péter, B. Tamain, and L. Valentin, J. Phys. Lett. 37, 1323 (1977).

[9]P. Glässel, R. S. Simon, R. M. Diamond, R. C. Jared, I. Y. Lee, L. G. Moretto, J. O. Newton, R. Schmitt, and F. S. Stephens, Phys. Rev. Lett. 38, 331 (1977).

[10]R. Albrecht, W. Dünnweber, G. Graw, H. Ho, S. G. Steadman, and J. P. Wurm, Phys. Rev. Lett. 34, 1400 (1975).

[11]J. B. Natowitz, M. N. Namboodiri, P. Kasiraj, R. Eggers, L. Adler, P. Gonthier, C. Cerruti, and T. Alleman, Phys. Rev. Lett. 40, 751 (1978).

[12]P. R. Christensen, F. Folkmann, Ole Hansen, O. Nathan, N. Trautner, F. Videbæk, S. Y. van der Werf, H. C. Britt, R. P. Chestnut, H. Freiesleben, and F. Pühlhofer, Phys. Rev. Lett. 40, 1245 (1978); Nucl. Phys. A349, 217 (1980).

[13]W. Trautmann, J. deBoer, W. Dünnweber, G. Graw, R. Kopp, C. Lauterbach, H. Puchta, and U. Lynen, Phys. Rev. Lett. 39, 1062 (1977); C. Lauterbach, W. Dünnweber, G. Graw, W. Hering, H. Puchta, and W. Trautmann, *ibid.* 41, 1774 (1978).

[14]C. F. Tsang, Phys. Scr. 10A, 90 (1974).

[15]K. Van Bibber, R. Ledoux, S. G. Steadman, F. Videbæk, G. Young, and C. Flaum, Phys. Rev. Lett. 38, 334 (1977).

[16]H. Puchta, W. Dünnweber, W. Hering, C. Lauterbach, and W. Trautmann, Phys. Rev. Lett. 43, 623 (1979).

[17]R. J. Puigh, H. Doubre, A. Lazzarini, A. Seamster, R. Vandenbosch, M. S. Zisman, and T. D. Thomas, Nucl. Phys. A336, 279 (1980).

[18]Y. Eyal, A. Gavron, I. Tserruya, Z. Fraenkel, Y. Eisen, S. Wald, R. Bass, G. R. Gould, G. Kreyling, R. Renfordt, K. Stelzer, R. Zitzmann, A. Gobbi, U. Lynen, H. Stelzer I. Rode, and R. Bock, Phys. Rev. Lett. 41, 625 (1978); Phys. Rev. C 21, 1377 (1980).

[19]D. Hilscher, J. R. Birkelund, A. D. Hoover, W. U. Schröder, W. W. Wilcke, J. R. Huizenga, A. C. Mignerey, K. L Wolf, H. F. Breuer, and V. E. Viola, Phys. Rev. C 20, 576 (1978).

[20]B. Tamain, R. Chechik, H. Fuchs, F. Hanappe, M. Morjean, C. Ngô, J. Péter, M. Dakowski, B. Lucas, C. Mazur, M. Ribrag, and C. Signarbieux, Nucl. Phys. A330, 253 (1979).

[21]H. Flocard, S. E. Koonin, and M. S. Weiss, Phys. Rev. C 17, 1682 (1978).

[22]G. B. Hagemann, Argonne National Laboratory Report No. ANL/PHY-79-4, 1979, p. 55.

[23]R. M. Diamond, Argonne National Laboratory Report No. ANL/PHY-79-4, 1979, p. 33.

[24]R. L. Kozub, N. H. Lu, J. M. Miller, D. Logan, T. W. Debiak, and L. Kowalski, Phys. Rev. C 11, 1497 (1975).

[25]J. Dauk, K. P. Lieb, and A. M. Kleinfeld, Nucl. Phys. A241, 170 (1975).

[26]B. B. Back, R. R. Betts, C. Gaarde, J. S. Larsen, E. Michelsen, and Tai Kuang-Hsi, Nucl. Phys. A285, 317 (1977).

[27]T. M. Cormier, A. J. Lazzarini, M. A. Neuhausen, A. Sperduto, K. Van Bibber, F. Videbæk, G. Young, E. B. Blum, L. Herreid, and W. Thoms, Phys. Rev. C 13, 682 (1976).

[28]G. Young, E. Blum. A. J. Lazzarini, M. A. Neuhausen, S. G. Steadman, and N. Tsoupas, in Proceedings of the Symposium on Macroscopic Features of Heavy-Ion Collisions, Argonne, 1976, edited by D. G. Kovar, Argonne National Laboratory Report No. ANL/PHY-76-2, 1979, p. 849.

[29]R. G. Markham, S. M. Austen, and H. Laumer, Nucl. Instrum. Methods 129, 141 (1975).

[30]L. C. Northcliffe and R. F. Schilling, Nucl. Data A7, 233 (1970).

[31]G. B. Hagemann, R. Broda, B. Herskind, M. Ishihara, S. Ogaza, and H. Ryde, Nucl. Phys. A245, 166 (1975).

[32]M. Ishihara, T. Numao, T. Fukuda, K. Tanaka, and I. Inamura, in Proceedings of the Symposium on Macroscopic Features of Heavy-Ion Collisions, Argonne, 1976, edited by D. G. Kovar, Argonne National Laboratory Report No. ANL/PHY-76-2, 1976, p. 617.

[33]B. P. Singh and H. C. Evans, Nucl. Instum. Methods 97, 475 (1971); E. Somorjai, *ibid.* 131, 557 (1975).

[34]M. M. Aleonard, G. J. Wozniak, P. Glässel, M. A. Deleplanque, R. M. Diamond, L. G. Moretto, R. P. Schmitt, and F. S. Stephens, Phys. Rev. Lett. 40, 622 (1978).

[35]A. Olmi, H. Sann, D. Pelte, Y. Eyal, A. Gobbi, W. Kohl, U. Lynen, G. Rudolf, H. Stelzer, and R. Bock, Phys. Rev. Lett. 41, 688 (1978).

[36]F. Rybicki, T. Tamura, and G. R. Satchler, Nucl. Phys. A146, 659 (1970).

[37]D. C. Camp and A. L. Van Lehn, Nucl. Instrum. Methods 76, 192 (1969).

[38]H. J. Rose and D. M. Brink, Rev. Mod. Phys. 39, 306 (1967).

[39]P. M. Endt and C. Van der Leun, Nucl. Phys. A214, 1 (1974).

[40]Monte Carlo statistical model code JULIAN, M. Hillman and Y. Eyal (unpublished).

[41]M. Sasagase, M. Sato, S. Hanashima, K. Furuno, Y. Nagashima, Y. Tagishi, S. M. Lee, and T. Mukumo, in Proceedings of the International Conference on Nuclear Physics, Berkeley, 1980, Lawrence Berkeley Laboratory Report LBL-11118, 1980, p. 527.

[42]J. R. Beene, O. Häusser, A. J. Ferguson, H. R. Andrews, J. A. Lone, B. Herskind, and C. Broude, Atomic Energy of Canada, Ltd., report, 1977 (unpublished).

[43]J. F. Mollenauer, Phys. Rev. 127, 867 (1962).

[44]R. A. Dayras, R. G. Stokstad, D. C. Hensley, M. L. Halbert, D. G. Sarantities, L. Westerberg, and J. H. Barker, Phys. Rev. C 22, 1485 (1980).

[45]R. D. Levine and S. G. Steadman, Phys. Lett 97B, 177 (1980).

[46]L. G. Moretto and R. P. Schmitt, Phys. Rev. C 21, 204 (1980).

[47]R. Vandenbosch, Phys. Rev. C 20, 171 (1979).

[48]Tai Kuang-Hsi, T. Døssing, C. Gaarde, and J. S. Larsen, Nucl. Phys. A316, 189 (1979).

[49]T. Inamura, M. Ishihara, T. Fukuda, and T. Shimioda, Phys. Lett. 68B 51 (1977).

[50]D. R. Zolnowski, H. Yamada, S. E. Cala, A. C. Kahler, and T. T. Sugihara, Phys. Rev. Lett. 41, 92 (1978).

[51]K. A. Geoffroy, D. G. Sarantities, M. L. Halbert, D. C. Hensley, R. A. Dayras, and J. H. Barker, Phys. Rev. Lett. 43, 1303 (1979); K. Siwek-Wilczyńska, E. H. du Marchie van Voorthuysen, J. van Popta, R. H. Siemssen, and J. Wilczyński, *ibid.* 42, 1599 (1979).